Interactions that Favor the Native over the Non-Native Disulfide Bond among Residues 58−72 in the Oxidative Folding of Bovine Pancreatic Ribonuclease A†

Robert P. Carty,‡ Matthew R. Pincus,§,|| and Harold A. Scheraga*,⊥

Department of Biochemistry, State University of New York Health Science Center, 450 Clarkson Avenue, Brooklyn, New York 11203, Department of Pathology, State University of New York Health Science Center, 450 Clarkson Avenue, Brooklyn, New York 11203, Department of Pathology and Laboratory Medicine, VA Medical Center, 800 Poly Place, Brooklyn, New York 11209, and Baker Laboratory of Chemistry and Chemical Biology, Cornell University, Ithaca, New York 14853-1301

Received August 16, 2002; Revised Manuscript Received October 7, 2002

ABSTRACT: In the initial stages of the oxidative folding of both bovine pancreatic ribonuclease A (RNase A) and a 58−72 fragment thereof from the fully reduced, denatured state, the 65−72 correctly paired disulfide bond forms in preponderance over the incorrectly paired 58−65 disulfide bond. Since both disulfide-bonded loops contain the same number of amino acid residues, the question arises as to whether the native pairing results from interactions within the 58−72 segment that lead to a nativelike structure even in its fully reduced form. To answer this question, the chain buildup procedure, based on ECEPP, including a solvation treatment, was used to generate the low-energy structures for the 58−72 RNase segment, beginning with residue 72 and building back to residue 58; in this fragment, all three Cys residues (at positions 58, 65, and 72) initially exist in the reduced (CysH) state. After the open-chain energy minima of the 65−72 peptide were generated, these conformations were allowed to form the 65−72 disulfide bond, and the energies of the resulting oxidized conformations were reminimized and rehydrated. The global minimum of the loop-closed 65−72 structure and many of the low-lying loop-closed minima could be superimposed on the energy-minimized X-ray structure for residues 65−72. The low-energy structures for the full open chain 58−72 peptide were then computed and were allowed to form disulfide bonds either between residues 65 and 72 (native) or between residues 58 and 65 (non-native), and their energies were reminimized and rehydrated in the loop-closed state. Although the overall fold of the 65−72 loop-closed global minimum was the same as for the energy-minimized X-ray structure of these residues, the overall rms deviation was 3.9 Å because of local deviations among residues 58−64. In contrast, the 65−72 segment of the global minimum of the 58−72 fragment could be superimposed on the corresponding residues of the energy-minimized X-ray structure. The lowest-energy structure for the 58−65 non-native paired 58−72 sequence was 6 kcal/mol higher in energy than that for the 58−72 peptide with the 65−72 disulfide bond formed. These results suggest that the native pairing of the 65−72 peptide arises from energetic determinants (adoption of left-handed single-residue conformations by Gly 68, and side chain interactions involving Gln 69) contained within this peptide sequence.

The oxidative folding of bovine pancreatic ribonuclease A is under investigation in our laboratories (*1*−*11*). In the early stages of oxidative folding with dithiothreitol, the dominant one-disulfide species contains the native disulfide bond between Cys 65 and Cys 72 (*12*). The next preponderant species contains the non-native disulfide bond between Cys 58 and Cys 65, the ratio of the populations of these species being approximately 4:1 in favor of the 65−72 bond. These two species constitute ∼50% of the 28 theoretically possible one-disulfide species, and each of the remaining 26 one-disulfide species is present to an extent of less than 10% (*12*). The 65−72 disulfide bond is also the dominant pair at later stages of oxidative folding, in both the two-disulfide (*13*) and three-disulfide (*14*) ensembles.

Interestingly, the 4:1 ratio of the 65−72 disulfide bond relative to the 58−65 disulfide bond is maintained not only in the full 124-residue protein but also in the oxidation of short reduced fragments containing only the three cysteine residues at positions 58, 65, and 72 (*15*−*17*). Since both the 58−65 and 65−72 loops contain the same number of residues, and are therefore essentially entropically equivalent, it appears that the preference for the native 65−72 disulfide-bonded loop may arise because of favorable enthalpic interactions within the 58−72 portion of the amino acid sequence, with relatively little influence from the surrounding residues. Identification of such interactions is the underlying goal in trying to understand the energetic basis for protein

† This work was supported by NIH Grant CA 42500 (M.R.P.), a VA Merit Review Grant (M.R.P.), a grant from the Lustgarten Foundation for Pancreatic Cancer Research (M.R.P.), and NIH Grant GM-24893 (H.A.S.). Support was also received from the National Foundation for Cancer Research (H.A.S.).

* To whom correspondence should be addressed.

‡ Department of Biochemistry, State University of New York Health Science Center.

§ Department of Pathology, State University of New York Health Science Center.

|| VA Medical Center.

⊥ Cornell University.

10.1021/bi0205350 CCC: $22.00
Published on Web 11/20/2002

folding, a process that was first demonstrated experimentally by Anfinsen (*18*). To provide insight into these observations, we have carried out conformational energy calculations to determine whether there is an energetic preference for forming the 65−72 disulfide bond compared to the 58−65 bond in a fragment consisting of residues 58−72.

MATERIALS AND METHODS

Computational Methods. All conformational energy calculations were carried out with ECEPP[1] (Empirical Conformational Energy Program for Peptides) (*19*). Solvation was taken into account with the hydration model of Hodes et al. (*20*, *21*). Briefly, residue hydration is a sum of specific and nonspecific free energies of hydration. Specific hydration arises from water molecules that are hydrogen bonded to polar atoms of the backbone and side chains of the amino acid residues in the sequence. The energy of this hydrogen bond is taken to be −1 kcal/mol. Nonspecific hydration pertains to the water molecules that can be packed around the side chains and backbone atoms of residues. Since the free energy of hydration of each of these groups is known, it is assumed that the free energy is partitioned equally among these waters. Depending on the reduction of the volume of water molecules that is excluded when two or more atoms approach each other, the nonspecific solvation free energy is computed as the fraction of the remaining water volume, multiplied by the free energy density of the group. All amino acid residues were treated as electrically neutral, with their atoms carrying partial charges. For a reference conformation, the free energy of the X-ray structure (*22*) was minimized; the resulting structure deviated by ∼0.1 Å from the experimental one.

Chain Buildup Procedure. To compute the low-energy conformations of the RNase A 58−72 peptide fragment (Cys-Ser-Gln-Lys-Asn-Val-Ala-Cys-Lys-Asn-Gly-Gln-Thr-Asn-Cys), we used the chain buildup procedure (*23*−*25*) with terminally blocked peptides, viz., with CH_3CO for the amino terminus and $NHCH_3$ for the carboxyl terminus of each peptide. Low-energy conformations for the oligopeptides were generated from the carboxyl terminus to the amino terminus, with the cysteine residues at positions 72, 65, and 58 in the CysH form. In this method, all combinations of conformations of the low-energy single-residue minima (*26*, *27*) for each successive residue were added to the growing chain and subjected to energy minimization.

The resulting low-energy minima at each stage of the buildup within a cutoff of 25 kcal/mol above the lowest-energy (global) minimum were retained. This high-energy cutoff was used because we have found that minima that have conformational energies that are more than 10 kcal/mol above the global minima in the absence of solvation can become the global minima after solvation is included.

The retained minima at each step were then subjected to hydration based on the solvation model of Hodes et al. (*20*, *21*). The solvation free energies were then resorted, and those conformations whose free energies were within 5 kcal/mol of that of the global minimum were retained. At this stage, we selected only the nondegenerate minima (*23*, *25*) from these resulting minima. Thus, if two or more conformations were found to have the same backbone conformation, only the lowest-energy conformation was retained. These nondegenerate minima were then combined with the single-residue minima of the next residue in the sequence, and the above process was repeated. The entire process was repeated iteratively, as each amino acid residue was added to the amino terminus of the growing chain, until all of the amino acids in the sequence had been included.

At the stage of the buildup procedure in which the low-energy minima for the 65−72 segment were calculated, each of these minima was allowed to undergo disulfide bond formation, using the ECEPP loop-closing potential (*19*), and the energies were then reminimized. These energy-reminimized structures were then subjected to the hydration procedure. The low-energy structures (that had energies that were within 5 kcal/mol of that of the global minimum) were superimposed on the energy-minimized X-ray structure (*22*) of the same residues in RNase A, by minimizing the root-mean-square (rms) deviation. The chain buildup procedure was then continued by addition of residues from position 64 back to position 58. In this procedure, the minima for the open (i.e., unpaired 65−72) chain form of residues 65−72 were used.

The minima generated for the 58−72 sequence were then subjected to disulfide loop closure either between residues 65 and 72 with Cys 58 as SH (native) or between residues 58 and 65 with Cys 72 as SH (non-native). These resulting conformations were then subjected to energy minimization and hydration as described for the 65−72 peptide in the preceding paragraph. The resulting low-energy conformations for the native disulfide-paired 58−72 peptide and for the 65−72 portion of these conformations were then superimposed on the corresponding energy-minimized X-ray structure for these residues.

RESULTS AND DISCUSSION

Lowest-Energy Conformations for the RNase A Peptide 65−*72*. The lowest-energy conformations for the terminally blocked peptide corresponding to residues 65−72 of RNase A (within 1 kcal/mol of the energy of the global minimum), with the disulfide loop closed, are shown in Table 1. The rms deviations of each of the generated low-energy structures from the energy-minimized X-ray structure are also shown in Table 1. It can be seen from this table that the global minimum (rms deviation of 2.3 Å) and a number of the energetically low-lying structures can be superimposed on the X-ray structure. The structure that gave the lowest rms deviation (2.2 Å), conformer 4 of Table 1, has an energy that is 0.4 kcal/mol higher than that for the global minimum (conformer 1 of Table 1). The global minimum structures, conformer 1 of Table 1, and conformer 4 of Table 1 are shown superimposed on the corresponding energy-minimized X-ray structure in panels A and B of Figure 1, respectively.

In the X-ray structure for residues 65−72 of RNase A, a type III bend forms among residues 65−68. When subjected to energy minimization and hydration, this structure was found to be >25 kcal/mol in energy above that for the global minimum (conformer 9 in Table 1). This relatively high energy arises in part from the presence of relatively high-

[1] Abbreviations: ECEPP, Empirical Conformational Energy Program for Peptides; RNase A, ribonuclease A.

Table 1: Low-Energy Minima for the Terminally Blocked RNase A 65−72 Peptide, *N*-Acetyl-Cys-Lys-Asn-Gly-Gln-Thr-Asn-Cys-$NHCH_3$[a]

	residues[b] and conformational states[c]								ΔE	rmsd
no.	C	K	N	G	Q	T	N	C	(kcal/mol)[d]	(Å)[e]
1	G	E	C	A*	D	A	C	A	0.0	2.3
2	G	E	C	D*	E	A	C	A	0.0	2.4
3	A	E	C	D*	E	A	F	C	0.3	2.4
4	A	A	C	C*	A	A*	A	A	0.4	2.2
5	G	E	C	A*	D	A	C	C	0.4	2.4
6	C	E	A	D*	A	F	F	A	0.7	3.2
7	E	D	C	C*	A	C	F	E	0.8	3.2
8	D	E	C	A*	G	E	F	C	1.1	3.4
9[f]	F	A	B	A*	F	B	B	F	26.0	0.0

[a] Minima with the 65−72 disulfide bond closed. [b] Represented by the single-letter amino acid code. [c] The single-letter conformational states that are listed are defined in ref *26*. [d] Conformational energies relative to that of the global minimum (no. 1 in the list), including the free energy of hydration. [e] The rms deviation for the superposition of the coordinates of all backbone atoms of each minimum energy structure on the coordinates of the corresponding atoms of the energy-minimized X-ray structure for these residues. [f] Energy-minimized X-ray structure (it deviates by ∼0.1 Å from the experimental X-ray structure).

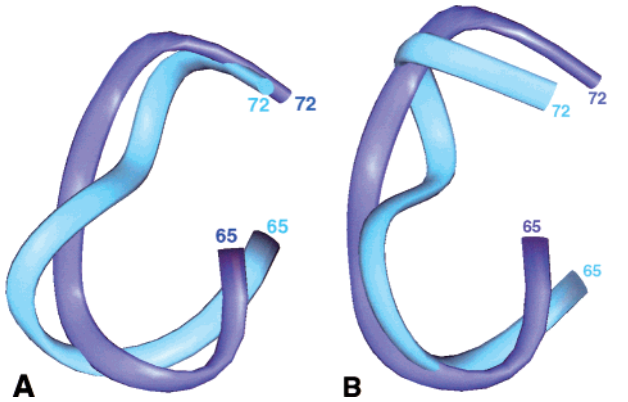

FIGURE 1: (A) Ribbon diagrams showing the superposition of the global minimum (conformer 1 in Table 1) for residues 65−72 of RNase A (light blue) on the X-ray structure for these residues (violet). (B) Ribbon diagram for the low-energy structure (conformer 4 in Table 1) (light blue) that gave the best fit to the X-ray structure (violet).

energy single-residue states such as B states for Asn 67, Thr 70, and Asn 71. Overall, the X-ray structure forms a bend at the Lys 66−Asn 67 junction, which is stabilized by a hydrogen bonding network between the side chains of Gln 69 and Asn residues 67 and 71. In the global minimum energy structure (conformer 1 of Table 1), there are two consecutive bends that form at residues 65−68 and 66−69. The second turn at positions 66−69, which occurs at the Asn 67−Gly 68 junction, causes some deviation of the chain from the X-ray structure but is similar to the NMR structure (*17*). The bend structure of the global minimum is stabilized by contacts made by the Gln 69 side chain, in particular a hydrogen bond between its side chain $CONH_2$ group and the backbone carbonyl oxygen of the CH_3CO end group preceding Cys 65.

Of all the low-energy structures that were generated, the one with the highest rms deviation (4 Å) (not shown) has an energy that was 3 kcal/mol higher than that for the global minimum. Thus, the global minimum and many energetically low-lying structures fold in a manner similar to that of the X-ray structure.

Table 2: Low-Energy Minima for the Terminally Blocked RNase A 58−72 Peptide, *N*-Acetyl-Cys-Ser-Gln-Lys-Asn-Val-Ala-Cys-Lys-Asn-Gly-Gln-Thr-Asn-Cys-$NHCH_3$[a]

	residues[b] and conformational states[c]															ΔE	rmsd
no.	C	S	Q	K	N	V	A	C	K	N	G	Q	T	N	C	(kcal/mol)[d]	(Å)[e]
1	C	E	A	A	C	A	A	A	A	E	C*	A	A*	A	A	0.0	2.4
2	E	G	F	A	A	A	A	A	A	E	C*	A	A*	A	A	0.0	2.6
3	C	F	A	C	A	A	A	A	A	C	C*	A	A*	A	A	0.0	2.5
4	E	A	A	C	A	A	A	A	A	C	C*	A	A*	A	A	1.0	2.5
5	D	G	F	A	A	A	A	A	A	E	C*	A	A*	A	A	1.0	2.6
6	C	E	A	A	C	A	A	A	A	E	C*	A	A*	A	A	1.0	2.6
7	C	G	F	A	A	A	A	A	A	E	C*	A	A*	A	A	1.0	2.6
8[f]	C	F	A	C	A	A	A	A	A	C	C*	A	A*	A	A	6.0	
9	F	A	G	E	A	A	A	A	A	C	C*	A	A*	A	A	6.0	
10	F	F	A	C	A	A	A	A	A	C	C*	A	A*	A	C	6.0	
11	E	F	A	C	A	A	A	A	A	E	C*	A	A*	A	A	6.0	
12	F	F	A	C	A	A	A	A	A	E	C*	A	A*	A	A	7.0	
13	C	A	G	E	A	A	A	A	A	C	C*	A	A*	A	A	7.0	
14[g]	G	B	F	C	C	E	F	F	A	B	A*	F	B	B	F	27.0	

[a] See footnote a of Table 1. [b] See footnote b of Table 1. [c] See footnote c of Table 1. [d] See footnote d of Table 1. [e] The rms deviation for the superposition of the coordinates of all backbone atoms of the eight carboxyl-terminal amino acids (residues 65−72) of each minimum energy structure on the coordinates of the corresponding atoms of the energy-minimized X-ray structure for these residues. [f] All minima for nos. 8−13 are for the 58−72 peptide with the *wrong* disulfide bond, i.e., between Cys 58 and Cys 65. [g] Energy-minimized X-ray structure (it deviates by ∼0.1 Å from the experimental X-ray structure).

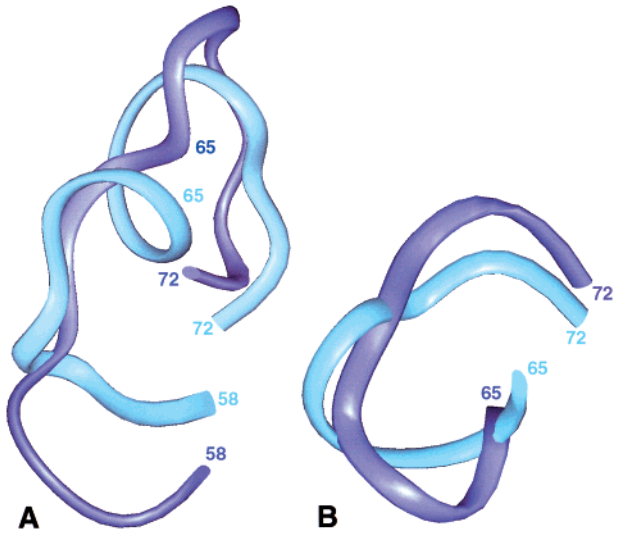

FIGURE 2: (A) Ribbon diagram for the superposition of the global minimum for residues 58−72 of RNase A (conformer 1 of Table 2) (light blue) on the X-ray structure for these residues (violet). (B) Ribbon diagram for the superposition of only residues 65−72 from the global minimum shown in panel A (light blue) on the corresponding X-ray structure for these residues (violet).

Lowest-Energy Conformations for the 58−72 RNase A Segment with the Disulfide Loop Closed between Cys 65 and Cys 72. The lowest-energy structures for the RNase A peptide Cys 58−Cys 72 with the Cys 65−Cys 72 disulfide bond are listed in Table 2. In this table, the rms deviations pertain to the superposition of residues 65−72 on the corresponding X-ray structure for these residues as discussed below in this section.

Superposition of the global minimum structure on the corresponding X-ray structure is shown in Figure 2A. While the overall chain folds are similar, the overall rms deviation is 4 Å, due mainly to differences in the structure in the middle of the chain. Unlike the X-ray structure, there is an α-helical

turn in the computed global minimum of the peptide from Val 63 to Lys 66. This helical structure was found to persist in all of the lowest-energy structures as shown in Table 2 (conformers 1−7) and Figure 2A.

Comparison of the conformational states in the low-energy conformations of residues 65 and 66 in the isolated 65−72 peptide (Table 1) with those of the same residues in the 58−72 peptide (Table 2) shows that these residues adopt the A, A conformation in the 58−72 peptide while they adopt different conformations (G, E) in the isolated peptide, with the exception of conformer 4 in Table 1 which does adopt the A, A conformation for residues 65 and 66. Since, as shown in Table 1, this structure could also be superimposed on the X-ray structure, we explored whether the 65−72 segment of the global minimum structure for the 58−72 peptide could be superimposed on the X-ray structure for these residues.

As shown in Table 2 (conformer 1) and Figure 2B, this domain could be superimposed on the X-ray structure with a slightly higher rms deviation than for the isolated 65−72 peptide. Thus, addition of the 58−64 segment appears to change the lowest-energy conformational states of the 65−72 segment but in such a way that this segment remains in a nativelike conformation since many of these conformers superimpose on the X-ray structure for these residues. Since the rms deviation is slightly higher, the presence of the 58−64 segment appears to destabilize the X-ray-like structure of this segment minimally.

Importantly, as noted in the first subsection above, in all of the low-energy conformations in Table 2 found for the global minimum conformation of the terminally blocked 65−72 peptide (conformer 1, Table 1 and Figure 1A), the side chain of Gln 69 hydrogen bonds to the carbonyl oxygen of the peptide group preceding Cys 65, thereby stabilizing both the Lys 66−Asn 67 and Asn 67−Gly 68 double bends in both conformer 1 in Table 1 and for the 65−72 segment of the 58−72 peptide (e.g., conformer 1 of Table 2 and Figure 2B). These results, therefore, implicate Gln 69 as being critical in stabilizing the bend structures of the 65−72 segment.

In a previous study (*16*), it was found that substitution of either Gln for Lys 66 or Ala for Asn 67 had no effect on the equilibrium constant for formation of the 65−72 disulfide bond for the 58−72 peptide. This result is compatible with our finding that the side chains of neither Lys 66 nor Asn 67 make stabilizing contacts in either of the computed lowest-energy structures for the 65−72 segment, i.e., as either the isolated peptide (conformer 1 of Table 1, Figure 1A) or as part of the 58−72 sequence (conformer 1 of Table 2, Figure 2B). Likewise, in the energy-minimized X-ray structure for residues 65−72 and 58−72 (conformer 9 of Table 1 and conformer 14 in Table 2, respectively), the side chain of Lys 66 makes no contacts with the other atoms in the chain. As noted in the first subsection above, the side chains of Asn 67 and Asn 71 hydrogen bond to the side chain of Gln 69. While substitution of Ala for Asn 67 would disrupt the Asn 67−Gln 69 hydrogen bond, it would not affect the Gln 69−Asn 71 hydrogen bond.

Inspection of Tables 1 and 2 reveals that Gly 68 adopts a left-handed (starred) state for all of the lowest-energy conformations. This conformation is found in bends with Gly at the second position (*28*) and suggests that it is also critical for forming a bend at the Asn (or Ala) 67−Gly 68 junction. On the basis of the above findings, therefore, Gly 68 and Gln 69 appear to be critical residues in stabilizing nativelike structures in the 65−72 sequence.

Lowest-Energy Structures for the 58−65 RNase A Segment with the Incorrect Disulfide Loop Closed between Cys 58 and Cys 65. When the open chain minima of peptide 58−72 were subjected to energy minimization with the 58−65 disulfide bond formed, the energies of the resulting lowest-energy conformations were found to be a minimum of 6 kcal/mol higher than the energy of the global minimum, as shown for lowest-energy conformers 8−13 (listed in Table 2). None of these structures could be superimposed on the X-ray structure for residues 58−72, the best rms fit being >5 Å. This suggests that disulfide loop closure favors the 65−72 disulfide bond energetically and is in qualitative agreement with the results of prior experimental studies that found that the 58−72 peptide, when allowed to oxidize from the fully reduced state, forms substantially more of the 65−72 oxidized species and that the equilibrium constant for formation of the 65−72 species is 4-fold greater than for formation of the 58−65 species (*15*, *16*).

Surprisingly, as shown in Table 2, many of the minima for this wrongly disulfide paired peptide adopt conformations for residues 65−72 that are similar to the minima found for the isolated 65−72 peptide. For example, in Table 2, conformers 8, 9, and 13 all adopt the AACC*AA*AA conformation for residues 65−72, which is identical to conformer 4 of Table 1. The latter conformer can be superimposed on the X-ray structure (rms deviation of 2.2 Å), as shown in Figure 1B. In this conformation, the S atoms of Cys 65 and Cys 72 are positioned so that they could form a disulfide bond.

Thus, despite the presence of the incorrect disulfide bond, the 65−72 segment still retains its nativelike structure. This result is in agreement with the prior experimental findings that the presence of neighboring residues 61−64, 73, and 74 have no influence on the ability of residues 65 and 72 to form a disulfide bond (*17*).

Other Methods for Computing Peptide Structure. Our conclusions follow from our computations based on the chain buildup procedure (*23*−*25*), using ECEPP potential functions (*19*). This method is based on a directed search, driven by the single-residue minima for each sequential amino acid that is added to the growing chain. This process automatically eliminates large high-energy regions of conformational space, and has resulted in the prediction of peptide structures that were in agreement with the experimentally determined ones (*29*).

However, it should be noted that many other potential functions, such as AMBER (*30*), CHARMM (*31*), and DISCOVER (*32*), have also proved to be successful in predicting peptide structure. In addition, other search methods have also been used successfully for predicting peptide structure; these involve computations that use the entire polypeptide chain in contradistinction to the chain buildup method that adds amino acids sequentially. Examples are molecular dynamics (*33*), simulated annealing (*34*), and Monte Carlo sampling with energy minimization (MCM) (*35*, *36*). Other searching approaches include lattice simulations of protein structure (*37*, *38*), genetic algorithms (*39*), homology modeling (*40*), and the electrostatically driven

Monte Carlo (EDMC) method (*41*). These methods are more suitable for simulations of whole protein structures rather than for smaller peptides such as the ones in this study.

CONCLUSIONS

The lowest-energy structures for the 65−72 peptide of RNase A are similar to the X-ray structure, although they deviate in the 66−69 region where the computed structures form a bend not present in the X-ray structure; it is stabilized by side chain interactions involving Gln 69 and by the adoption of left-handed single-residue states by Gly 68. This result is in agreement with the results of NMR studies in which a bend was found for residues 66−69 in the solution structure for the 65−72 peptide (*17*). The lowest-energy minima for the full 58−72 peptide cannot be completely superimposed on the X-ray structure for the corresponding residues, due mainly to helix formation for residues 63−66 in the low-energy minima for this peptide. However, while the 58−64 segment changes the conformational preferences for residues 65−72, the lowest-energy structures for this segment in the full 58−72 peptide still retain a nativelike conformation, although slightly less so than for the isolated peptide. That the 65−72 segment has strong local conformational determinants that dictate the formation of a 65−72 disulfide bond is demonstrated by the fact that, despite formation of the wrong 58−65 disulfide bond, the low-energy states for the 65−72 segment are nativelike with Cys 65 and 72 positioned to form a disulfide.

The lowest-energy structures for the 58−72 peptide suggest that the presence of residues 58−64 appears to destabilize the nativelike 65−72 structure slightly, although this effect is minimal, as discussed in the preceding paragraph. Residues 58−64 differ in conformation from those of the X-ray structure (Figure 2A). Our results, therefore, suggest that formation of the correct 65−72 disulfide bond is driven by local interactions within the 65−72 segment. In the full RNase A molecule, Cys 58 is paired to Cys 110. Thus, with Cys 58 and its near-neighbor residues placed near a structurally well defined domain [chain folding initiation site (*42*)] involving residues 105−124 in the X-ray structure, the conformational preferences of residues 58−64 may be influenced by long-range interactions with this C-terminal domain.

REFERENCES

1. Carty, R. P., Gerewitz, F., and Pincus, M. R. (1982) *Biophys. J. 37*, 95A.
2. Rothwarf, D. M., Li, Y. J., and Scheraga, H. A. (1998) *Biochemistry 37*, 3760−3766.
3. Rothwarf, D. M., Li, Y. J., and Scheraga, H. A. (1998) *Biochemistry 37*, 3767−3776.
4. Iwaoka, M., Juminaga, D., and Scheraga, H. A. (1998) *Biochemistry 37*, 4490−4501.
5. Xu, X., and Scheraga, H. A. (1998) *Biochemistry 37*, 7561−7571.
6. Welker, E., Narayan, M., Volles, M. J., and Scheraga, H. A. (1999) *FEBS Lett. 460*, 477−479.
7. Wedemeyer, W. J., Welker, E., Narayan, M., and Scheraga, H. A. (2000) *Biochemistry 39*, 4207−4216.
8. Narayan, M., Welker, E., Wedemeyer, W. J., and Scheraga, H. A. (2000) *Acc. Chem. Res. 33*, 805−812.
9. Scheraga, H. A., Wedemeyer, W. J., and Welker, E. (2001) *Methods Enzymol. 341*, 189−221.
10. Welker, E., Narayan, M., Wedemeyer, W. J., and Scheraga, H. A. (2001) *Proc. Natl. Acad. Sci. U.S.A. 98*, 2312−2316.
11. Welker, E., Wedemeyer, W. J., Narayan, M., and Scheraga, H. A. (2001) *Biochemistry 40*, 9059−9064.
12. Xu, X., Rothwarf, D. M., and Scheraga, H. A. (1996) *Biochemistry 35*, 6406−6417.
13. Volles, M. J., Xu, X., and Scheraga, H. A. (1999) *Biochemistry 38*, 7284−7293.
14. Wedemeyer, W. J., Xu, X., Welker, E., and Scheraga, H. A. (2002) *Biochemistry 41*, 1483−1491.
15. Milburn, P. J., and Scheraga, H. A. (1988) *J. Protein Chem. 7*, 377−398.
16. Altmann, K.-H., and Scheraga, H. A. (1990) *J. Am. Chem. Soc. 112*, 4926−4931.
17. Talluri, S., Falcomer, C. M., and Scheraga, H. A. (1993) *J. Am. Chem. Soc. 115*, 3041−3047.
18. Anfinsen, C. B. (1973) *Science 181*, 223−230.
19. Némethy, G., Gibson, K. D., Palmer, K. A., Yoon, C. N., Paterlini, G., Zagari, A., Rumsey, S., and Scheraga, H. A. (1992) *J. Phys. Chem. 96*, 6472−6484.
20. Hodes, Z. I., Némethy, G., and Scheraga, H. A. (1979) *Biopolymers 18*, 1565−1610.
21. Hodes, Z. I., Némethy, G., and Scheraga, H. A. (1979) *Biopolymers 18*, 1611−1634.
22. Wlodawer, A., Svensson, L. A., Sjölin, L., and Gilliland, G. L. (1988) *Biochemistry 27*, 2705−2717.
23. Scheraga, H. A. (1984) *Carlsberg Res. Commun. 49*, 1−55.
24. Vasquez, M., and Scheraga, H. A. (1988) *J. Biomol. Struct. Dyn. 5*, 705−755.
25. Pincus, M. R. (1988) *Int. J. Quantum Chem., Quantum Biol. Symp. 15*, 209−220.
26. Zimmerman, S. S., Pottle, M. S., Némethy, G., and Scheraga, H. A. (1977) *Macromolecules 10*, 1−9.
27. Vasquez, M., Némethy, G., and Scheraga, H. A. (1983) *Macromolecules 16*, 1043−1049.
28. Pincus, M. R., van Renswoude, J., Harford, J. B., Chang, E. H., Carty, R. P., and Klausner, R. D. (1983) *Proc. Natl. Acad. Sci. U.S.A. 80*, 5253−5257.
29. Vasquez, M., Némethy, G., and Scheraga, H. A. (1994) *Chem. Rev. 94*, 2183−2239.
30. Weiner, S. J., Kollman, P. A., Case, D. A., Singh, V. C., Ghio, C., Alagona, G., Profeta, S., and Weiner, P. K. (1986) *J. Am. Chem. Soc. 108*, 765−784.
31. Brooks, B. R., Bruccoleri, R. E., Olafson, B. D., States, D. J., Swaminathan, S., and Karplus, M. (1983) *J. Comput. Chem. 4*, 187.
32. Dauber-Osguthorpe, P., Roberts, V. A., Osguthorpe, D. J., Wolff, J., Genest, M., and Hagler, A. T. (1988) *Proteins: Struct., Funct., Genet. 4*, 31−47.
33. Brooks, C. L., III, and Case, D. A. (1993) *Chem. Rev. 93*, 2487.
34. Kirkpatrick, S., Gelatt, C. D., and Vecci, M. P. (1983) *Science 220*, 671.
35. Li, Z., and Scheraga, H. A. (1987) *Proc. Natl. Acad. Sci. U.S.A. 84*, 6611−6615.
36. Saunders, M. J. (1989) *J. Comput. Chem. 10*, 203.
37. Covell, D. G., and Jernigan, R. L. (1990) *Biochemistry 29*, 3287.
38. Godzik, A., Kolinski, A., and Skolnick, J. (1993) *J. Comput. Chem. 14*, 1194.
39. Forest, S. (1993) *Science 261*, 872.
40. Rose, J., and Eisenmenger, F. (1991) *J. Mol. Evol. 32*, 340.
41. Ripoll, D. R., and Scheraga, H. A. (1988) *Biopolymers 31*, 319.
42. Matheson, R. R., Jr., and Scheraga, H. A. (1978) *Macromolecules 11*, 819−829.

BI0205350